ACS APPLIED MATERIALS & INTERFACES

Letter

Cite This: ACS Appl. Mater. Interfaces 2018, 10, 30051−30057

www.acsami.org

Sunlike White-Light-Emitting Diodes Based on Zero-Dimensional Organic Metal Halide Hybrids

Michael Worku,[†] Yu Tian,[†] Chenkun Zhou,[‡] Sujin Lee,[‡] Quinton Meisner,[§] Yan Zhou,[§] and Biwu Ma*[,†,§]

[†]Materials Science and Engineering Program and [§]Department of Chemistry and Biochemistry, Florida State University, Tallahassee, Florida 32306, United States

[‡] Department of Chemical and Biomedical Engineering, FAMU-FSU College of Engineering, Tallahassee, Florida 32310, United States

Supporting Information

ABSTRACT: Here we report ultraviolet (UV)-pumped white-light-emitting diodes (WLEDs) with sunlike full spectrum emissions, by using a commercially available blue phosphor ($BaMgAl_{10}O_{17}:Eu^{2+}$) and a series of broadband zero-dimensional (0D) organic metal halide hybrids as down conversion phosphors. By controlling the blend ratio of phosphors, we have achieved high-quality WLEDs with excellent general color rendering index (CRI R_a) of up to 99 and deep-red rendering index (R9) of up to 99. These WLEDs exhibiting white emissions with correlated color temperatures (CCTs) ranging from 3000 to 6000 K perfectly mimic sunlight at different times of day.

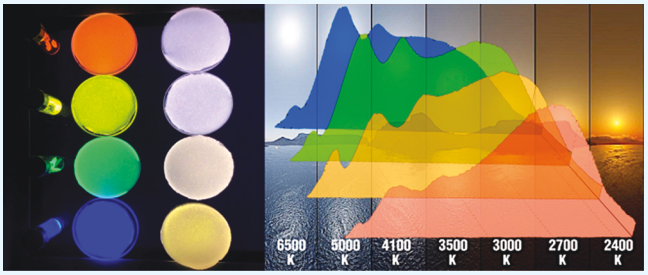

KEYWORDS: *white LED, organic metal halide hybrid, down conversion phosphor, high color rendering index, solid-state lighting*

The lighting industry has changed significantly over the past decade with light-emitting-diode (LED) technology becoming the mainstream for its long lifetime, low carbon emission, and high efficiency. To date, there are mainly two approaches for LEDs to achieve white-light emission.[1] The first approach, combining red, green, and blue LEDs, is not well-adapted commercially, as it suffers from cumbersome fabrication, power-dependent spectral variation, thermal instability, and differential aging-induced chromatic instability.[1] The second approach, which can be subdivided into two categories, partial conversion and full conversion,[2] involves the use of a blue or UV-LED and a phosphor layer to convert short wavelength light into longer ones to produce white light. This down conversion approach has been widely used for commercial white LEDs (WLEDs), because of the ease of manufacturing as well as thermal and flux independent chromatic stability. However, blue LED based WLEDs often have poor color rendering due to spectral discontinuity and have also been found to cause damage to retinal photoreceptors that mediate the circadian rhythm in mammals.[3]

To fabricate WLEDs with excellent color rendering, the full conversion method, using a UV-LED with multiple phosphors, is an effective approach. Several groups have reported UV pumped WLEDs with ultrahigh CRI of more than 95, by employing multiple phosphors[4−6] and semiconductor quantum dots (QDs).[7,8] Despite suffering from fundamental losses due to quantum deficit,[9] UV pumped WLEDs are preferred for high CRI applications over blue LED pumped WLEDs, because of their good chromatic stability and easy color tunability.[10] However, most down-conversion phosphors developed to date, including rare earth and transition metal doped/activated phosphors,[11−16] semiconductor QDs,[17−22] organic dyes[23,24] and more recently halide perovskite nanocrystals,[25−29] suffer from nonideal photoluminescence quantum efficiency (PLQE), strong reabsorption losses, expensive and time-consuming synthesis, as well as material toxicities, for instance, Cd based QDs and Pb based halide perovskite nanocrystals. To overcome losses from reabsorption of emitted light, multiple approaches have been proposed including co-doping of luminescent activators into a single phosphor,[30] using giant core−shell QDs[31] and core−multishell semiconductor QDs[32,33] as well as doping core−shell QDs to obtain large Stokes shift.[34] However, dopant-concentration-dependent energy transfer between dopant ions was prevalent for triply codoped phosphors.[30]

An ideal down-converter, as defined by Smet et al., should have near-unity PLQE, excitation overlapping with the emission of the pumping LED, and excellent thermal and photostability in addition to enabling good color rendering.[9] Our group recently reported a series of zero-dimensional (0D) organic metal halide hybrids exhibiting strongly Stokes-shifted broadband emission with near-unity PLQEs.[35−37] With the photoactive metal halide species periodically doped within the

Received: July 23, 2018
Accepted: August 28, 2018
Published: August 28, 2018

DOI: 10.1021/acsami.8b12474
ACS Appl. Mater. Interfaces 2018, 10, 30051−30057

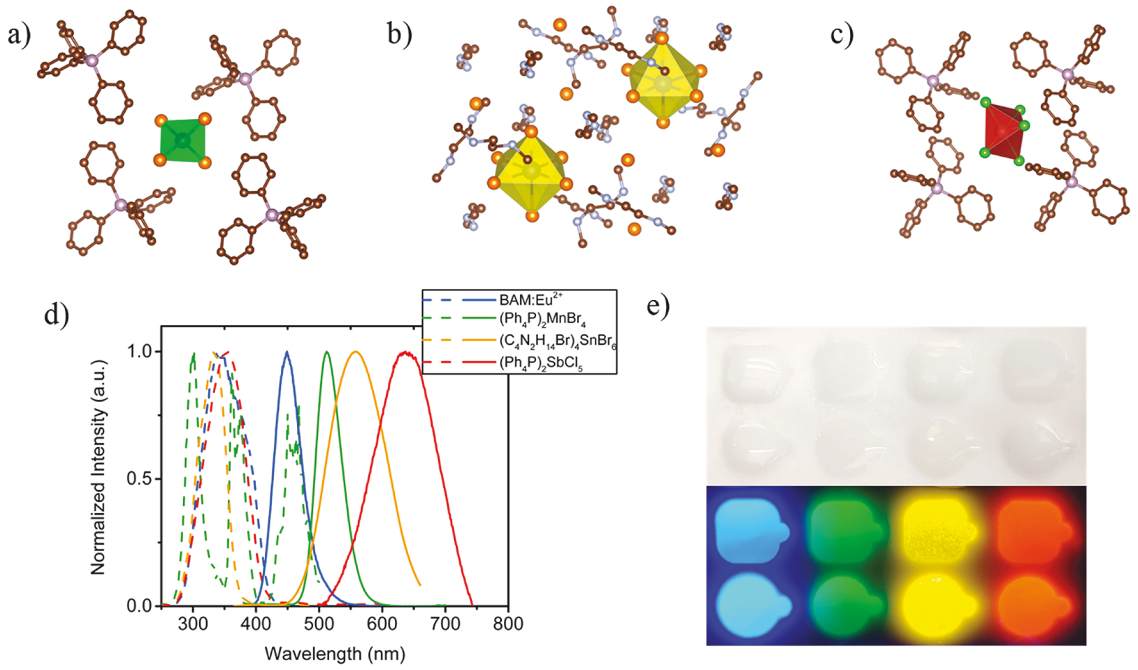

Figure 1. View of individual (a) $MnBr_4^{2-}$ tetrahedron surrounded by Ph_4P^+cations, (b) $SnBr_6^{4-}$ octahedra surrounded by $C_4N_2H_{14}Br^+$ cations, and (c) $SbCl_5^{2-}$ pyramid surrounded by Ph_4P^+cations (green, yellow, and red polyhedra: $MnBr_4^{2-}$ tetrahedron, $SnBr_6^{4-}$ octahedra, and $SbCl_5^{2-}$ pyramid; orange spheres: Br^- ions; green spheres: Cl^- ions; purple spheres: phosphorus atoms; blue spheres: nitrogen atoms; brown spheres: carbon atoms); (d) excitation (dashed lines) and emission (solid lines) of phosphors; (e) 0D hybrid crystals in polydimethylsiloxane (PDMS) gel under ambient light and under UV irradiation.

organic network, a large Stokes shift was observed because of excited-state structural reorganization. There was an effort to make UV pumped WLEDs by combining a yellow emitting 0D organic metal halide hybrid $(C_4N_2H_{14}Br)_4SnBr_xI_{6-x}$ (x = 3) with a commercially available blue phosphor $BaMgAl_{10}O_{17}:Eu^{2+}$ ($BAM:Eu^{2+}$), but the highest CRI was limited to 85.[36] Recently, a green emitting 0D organic metal halide hybrid was reported with a similar, albeit smaller, Stokes shift.[38] Because of their inert nature, the earth abundance of raw materials, and the facile synthesis at room temperature, these new phosphors have the potential to provide a nontoxic, high-stability, and lower-cost solution, outperforming commercial rare-earth-doped inorganic phosphors and heavy-metal based QDs.

Here we report a series of UV-pumped WLEDs, in which $BAM:Eu^{2+}$ is used as a blue phosphor, and a series of 0D organic metal halide hybrids, $(Ph_4P)_2MnBr_4$, $(C_4N_2H_{14}Br)_4SnBr_6$, and $(Ph_4P)_2SbCl_5$, as green, yellow, and red phosphors, respectively. These WLEDs can produce full spectrum white light that approximates halogen or incandescent lighting and natural daylight, with extremely high CRIs of up to 99, excellent deep-red color rendering, R9s of up to 99, and superior color quality scale (CQS) values. By carefully controlling the phosphor blend ratios, white emissions with different correlated color temperatures (CCTs), ranging from 3000 to 6000 K, have been demonstrated, which perfectly mimic sunlight at different times of day. The thermal and current stability of the CCT and Commission Internationale de l'Eclairage (CIE) chromaticity coordinates of the devices have also been investigated.

$(C_4N_2H_{14}Br)_4SnBr_6$ and $(Ph_4P)_2SbCl_5$ were synthesized following the previously reported procedures.[35,37] $(Ph_4P)_2MnBr_4$ crystals were prepared via a modified procedure, by diffusing $(C_2H_5)_2O$ into a 2:1 ratio solution of Ph_4PBr and $MnBr_2$ in dimethylformamide (DMF) overnight. This procedure gave a higher product yield and produced larger crystals compared to the previously reported method by Xu et al.[38] As can be gathered from the crystal structures, Figure 1a–c, 0D organic metal halide hybrids differ from their higher dimensional counterparts because the photoactive polyhedra are completely isolated from each other by the bulky wide bandgap organic cations, thereby inhibiting electronic band formation between luminescent centers. This arrangement allows 0D organic metal halide hybrids to display the intrinsic properties of individual metal halide polyhedra in the bulk crystal with a near-unity PLQE. Moreover, because of molecular excited-state structural reorganization, broad emission and large Stokes shift are characteristic of this class of materials. Additionally, the organic cations also function as shells to the photoactive metal halide cores, providing stability against moisture and oxidizing agents.

The photophysical properties of the four phosphors, blue-emitting $BAM:Eu^{2+}$, green-emitting $(Ph_4P)_2MnBr_4$, yellow-emitting $(C_4N_2H_{14}Br)_4SnBr_6$, and red-emitting $(Ph_4P)_2SbCl_5$, were characterized using steady-state photoluminescence and UV–vis absorption spectroscopy. The results are summarized in Table S1. The 0D organic metal halide hybrids generally show broad emissions, as illustrated in Figure 1d, with calculated full width at half-maximum (fwhm) of 48 nm (0.22 eV), 108 nm (0.43 eV), and 118 nm (0.36 eV) for $(Ph_4P)_2MnBr_4$, $(C_4N_2H_{14}Br)_4SnBr_6$, and $(Ph_4P)_2SbCl_5$, respectively. These broadband emissions have clear advantages over narrow emissions from QDs and typical 3D metal halide perovskites for the realization of full spectrum white emission. Moreover, as shown in Figure 1d, the excitation spectra of all four phosphors peak at similar short wavelengths between 330 and 370 nm. The absorption spectra of three of the four phosphors also never extend into the visible range beyond 400

DOI: 10.1021/acsami.8b12474
ACS Appl. Mater. Interfaces 2018, 10, 30051–30057

nm, as depicted in Figure S1. Only $(Ph_4P)_2MnBr_4$ displays three different absorption peaks at 300 nm, 350 and 460 nm due to energy splitting of the $^4T_1$ excited state of the Mn(II) ion.[18] However, the absorption coefficient at 460 nm is miniscule resulting in a negligible reabsorption of blue emission. The Stokes shifts were calculated to be 115 nm (0.84 eV), 52 nm (0.27 eV), 205 nm (1.28 eV), and 283 nm (1.56 eV) for BAM:Eu^{2+}, $(Ph_4P)_2MnBr_4$, $(C_4N_2H_{14}Br)_4SnBr_6$ and $(Ph_4P)_2SbCl_5$, respectively. These large Stokes shifts are instrumental in fabricating WLEDs with little-to-no efficiency loss from reabsorption of emitted light. The PLQEs of the commercial blue phosphor BAM:Eu^{2+}, and 0D organic metal halide hybrid crystals $(Ph_4P)_2MnBr_4$, $(C_4N_2H_{14}Br)_4SnBr_6$ and $(Ph_4P)_2SbCl_5$ were reported to be as high as 93%, 97%, 95%, and 87%, respectively.[35,37−39] These results indicate that the 0D organic metal halide hybrids possess broad emissions, strong excitation in the UV region, large Stokes shifts and high PLQEs suitable for application in high color rendering, full-spectrum UV pumped efficient WLEDs with negligible reabsorption losses.

To fabricate optically pumped WLEDs, we first investigated ways of embedding phosphors into polymer matrices to prepare phosphor−polymer composites. The typical procedure involved grinding single-crystal phosphors into fine powders, encapsulating ground phosphors in an inert polymer matrix, and attaching the phosphor−polymer composite to a commercial UV-LED. Two routes were explored to reduce single crystals to powders: hand grinding using mortar and pestle and planetary ball milling. Although particle sizes of approximately 300 nm were obtained through planetary ball-milling, the PLQEs were significantly reduced compared to those of the single crystals, as illustrated in Figure S2. This is likely because the larger surface area to volume ratio of ball-milled powders leads to increased oxidation and moisture adsorption. The largest PLQE reduction was observed for $(C_4N_2H_{14}Br)_4SnBr_6$, most likely because of the oxidation of Sn^{2+} to Sn^{4+}. Despite producing larger size particles, hand ground phosphors maintained reasonable PLQEs and thus were employed in phosphor-polymer composite preparation and device fabrication. Silicone and epoxy are the most widely used polymer matrices for phosphor encapsulation. The EI-1184 polydimethylsiloxane (PDMS) was found to possess all the desirable qualities of an inert polymer matrix such as transparency in the UV−visible light spectrum, inertness and stability under various operating conditions, and thus was chosen as an encapsulant. Another silicone variant, Sylgard-184 PDMS, led to significant PLQE reduction due to the interaction between the platinum-based catalyst and 0D organic metal halide hybrids during Pt-catalyzed hydrosilylation of PDMS. A proprietary epoxy resin, EPO-TEK 305, was also found to considerably quench emission from the 0D organic metal halide hybrids. Figure 1e shows a photo of phosphor doped PDMS polymer composites under ambient light and UV irradiation. The colorless phosphor-polymer composites under ambient light are consistent with the little-to-no absorption of these phosphors in the visible region. The strong photoluminescence of the composites under UV irradiation matches perfectly with that of single crystals.

As discussed above, color rendering is one of the most crucial figures of merit for WLEDs and has been the topic of several studies. To produce white light with optimum color rendering and tunable CCT, we performed color mixing simulations. This was accomplished by first fabricating monochromatic LEDs and then combining the spectra to yield ultrahigh color rendering white light. Employing the Osram-Sylvania Color Calculator software, color rendering values, CRI and CQS, were optimized for four different CCT values, 3000, 4000, 5000, and 6000 K. These CCT values were chosen because they represent the range of color temperatures typical in solid-state lighting applications, from warm white (3000 K) for residential lighting to cold white (6000 K) for commercial and industrial venues. The simulation results, given in the Table S2, revealed that ultrahigh color rendering, CRI and CQS in the range of 98−99, could be achieved. However, of the recommended 14 reflective test-color samples, CRIs of only the first eight, R1−R8, are used to calculate the general CRI (R_a) value.[40] And neglecting the R9 value, the quantity representing the deep-red color rendering, can yield a high R_a white light with inaccurate rendering of deep-red regions. R9 values of commercial WLEDs are usually limited to below 30 and reports of high R9 values are very rare. The simulation carried out, however, produced R9 values as high as 99. Color rendering values of this magnitude are seldom reported in the literature. Even more significant, the color rendering is relatively insensitive to variations in CCT. This indicates that WLEDs based on these phosphors can be used for high color rendering applications in any arena, be it residential or industrial. In contrast, the most typical commercial white LED based on YAG:Ce^{3+} phosphor has poor color rendering at lower CCTs, R_a of 70, and little flexibility in CCT tuning.[41]

The simulation results showed weight ratios of 1:2.7:3.6:9, 1:3:4.5:3.5, 1:3.3:4:3, and 1:2.5:3:2 for BAM:Eu^{2+}:$(Ph_4P)_2MnBr_4$:$(C_4N_2H_{14}Br)_4SnBr_6$:$(Ph_4P)_2SbCl_5$, would yield 3000, 4000, 5000, and 6000 K CCT white light, respectively. The phosphors were then carefully blended according to the simulation results and encapsulated in PDMS to produce the white-light-emitting phosphor-polymer composites. By directly attaching these phosphor layers to an Opulent 365 nm UV-LED, we were able to fabricate WLEDs. Emission spectra of the devices were collected under forward bias current of 20 mA using a Keithley 2400 source-meter and an Ocean Optics USB4000 spectrometer. The photometry values, summarized in Table 1, were calculated from the emission spectra using the Osram-Sylvania color calculator software. These experimental results confirm the ultrahigh color rendering that can be achieved, as evidenced by the R_a, CQS, and R9 values. Moreover, this excellent color rendering was maintained across widely varying CCTs making these devices viable for a wide range of solid-state lighting applications. The comparison between experimental results and simulated and blackbody radiator spectra at corresponding color temperatures reveals the uncanny similarity in both shape and breadth, as shown in Figure 2a−d. And thus, the excellent color rendering property of white emissions from these prototype devices stems from their exceptional resemblance

Table 1. Prototype Device Photometry Characterization Results

CCT	CRI (R_a)	CQS	R9	CIE (x, y)
2982 K	92	96	81	(0.4218, 0.3710)
4028 K	99	99	99	(0.3782, 0.3722)
5061 K	93	97	73	(0.3426, 0.3406)
5850 K	98	97	94	(0.3251, 0.3317)

DOI: 10.1021/acsami.8b12474
ACS Appl. Mater. Interfaces 2018, 10, 30051−30057

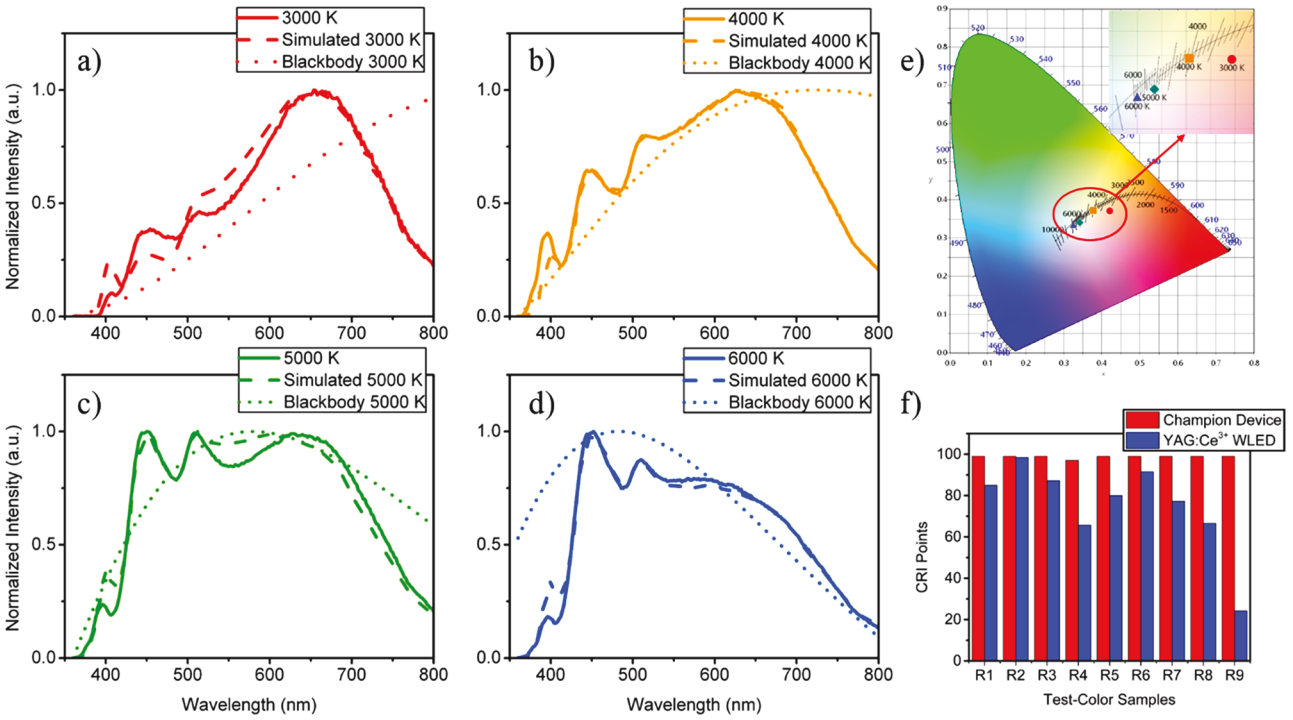

Figure 2. Emission spectra of prototype devices, simulated white light, and blackbody radiators at (a) 3000, (b) 4000, (c) 5000, and (d) 6000 K CCT; (e) CIE 1931 diagram showing the chromaticity points of prototype devices; inset, CIE coordinates of devices lie on or close to the Planckian locus; (f) CRI comparison between the champion 4000 K device and a YAG:Ce^{3+}-based commercial white LED.[42].

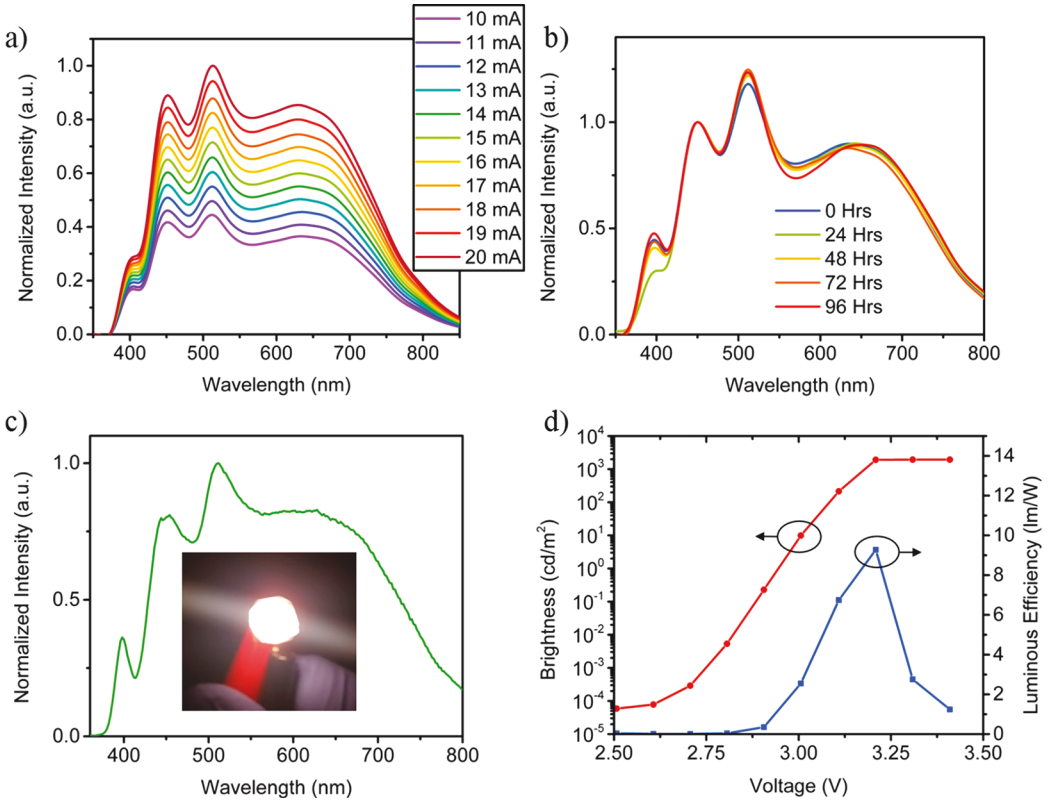

Figure 3. (a) Electroluminescence under varying forward bias current from 10 to 20 mA; (b) electroluminescence of devices after aging at 85 °C for 0 to 96 h; (c) emission spectrum of the prototype device used for efficiency measurement; inset: prototype device under operation; (d) voltage versus brightness and luminous efficiency of prototype device.

to emission from a blackbody radiator. Calculated CIE coordinates of the devices, as shown in Figure 2e, are also almost in-line with the Planckian locus, reaffirming that these devices perfectly mimic the emission of a blackbody radiator.

DOI: 10.1021/acsami.8b12474
ACS Appl. Mater. Interfaces 2018, 10, 30051−30057

Our champion device, labeled 4000 K, has R_a, CQS, and R9 of 99 at a CCT of 4028 K. Figure 2f illustrates the CRI comparison between the champion 4000 K device and a YAG:Ce^{3+} based commercial WLED. To the best of our knowledge, WLEDs exhibiting such high R_a, CQS and R9 with such precise control and tunability of CCT have not been reported yet.

Thermal stability of the phosphors was investigated using a temperature controller fitted spectrophotometer. The results, shown in Figure S3a–d, were collected in the forward direction, by first increasing the temperature to 80 °C at 20 °C steps and in the reverse direction, by decreasing the temperature back to 20 °C at 20 °C steps. Except for $(C_4N_2H_{14}Br)_4SnBr_6$, the results show similar trends of slight decrease in photoluminescence intensity upon increasing the temperature. The highest intensity loss was recorded for $(Ph_4P)_2SbCl_5$ at 80 °C, retaining about 62% of the room temperature photoluminescence intensity. Moreover, a slight blue-shifting of the emission peak was also observed. This is likely because of temperature induced bond stretching resulting in smaller Stokes shift than the one observed at room temperature. The commercial blue phosphor BAM:Eu^{2+} and the green emitting $(Ph_4P)_2MnBr_4$ retained 90% and 92% of their initial room temperature photoluminescence intensity, respectively. This is not surprising because the BAM:Eu^{2+} phosphor only experiences significant oxidation induced thermal degradation for temperatures above 500 °C.[43] The emission from $(C_4N_2H_{14}Br)_4SnBr_6$, however, showed an increase in intensity with increasing temperature. This anomaly was addressed by Zhou et al. as arising from increased absorption at higher temperatures.[35] Measurement in the reverse direction showed excellent recovery of photoluminescence intensity for all phosphors.

Stability of the white light emission under variation of forward bias current was also investigated. In this experiment, the emission of a test device was recorded for the forward bias current range of 10 to 20 mA with 1 mA step. The result of this experiment, illustrated in Figure 3a, shows that the shape of the spectrum does not experience any significant changes. The CRI (R_a) of the device increased from 94 at 10 mA to 96 at 20 mA. A slight shift in CIE coordinates was also observed going from (0.3264, 0.3395) at 10 mA to (0.3354, 0.3506) at 20 mA, as depicted in the Figure S4a. Nonetheless, a linear increase in irradiance with increasing current was observed without significant effect on the photometric characteristics of the white light generated. Because of the heat generated by the pump LED, we also found it necessary to test the chromatic stability of the phosphor layer under thermal strain. A batch of devices were fabricated and aged at 85 °C for 24, 48, 72, and 96 h under ambient atmosphere. The white emissions from these layers, illustrated in Figure 3b, were normalized by the intensities of the blue peak at 450 nm, because, as discussed above, the commercial blue phosphor has a thermally robust emission. The CIE chromaticity coordinate was shifted from (0.3254, 0.3448) before aging to (0.3195, 0.3423) after 96 h in the oven at 85 °C, as illustrated in Figure S4b. The largest coordinate shift was −0.0059, well within the industry standard of $\Delta \pm 0.01$.[44]

The efficiency of a model WLED, electroluminescence spectrum shown in Figure 3c, with 5217 K CCT, 99 CRI (R_a) and 96 R9 was studied. The device was operated under forward bias current of up to 105 mA using a Keithley 2400 source-meter. The resulting optical power and photocurrent were measured using a Newport 818-UV photodetector and a Newport multifunction optical meter. To eliminate contributions to photocurrent from the pump UV-LED, we used an Edmund Optics deep-dyed polyethylene terephthalate (PET) UV filter. Only emission in the forward direction was collected during this measurement. As can be seen from Figure 3d, brightness values of up to 1935 cd m^{-2} and luminous efficiency of up to 9.73 lm W^{-1} were obtained. Moreover, further calculation showed an external quantum efficiency (EQE) of 5.7% and current efficiency of 9 cd A^{-1}, as depicted in the Figure S5. However, emission in the forward direction accounts for approximately one-fourth of the total out-coupled optical power because of strong waveguiding.[45] Thus, measurement of the luminous efficiency in an integrating sphere would likely yield values up to 40 lm W^{-1}. Additionally, further refinement in processing would most likely improve the present efficiency values. Particularly, solving the particle size reduction and inert encapsulation problems would probably lead to a significant increase in device efficiency.

In summary, we have demonstrated the use of a series of 0D organic metal halide hybrids together with a commercially available blue phosphor BAM:Eu^{2+} for the fabrication of sunlike full spectrum WLEDs with near perfect CRI values. These 0D organic metal halide hybrids made of earth-abundant elements possess numerous features desired for application as down conversion phosphors, including facile synthesis, near-unity PLQE, broadband emission, and large Stokes shift. To the best of our knowledge, our prototype WLEDs, consisting of a polymer film doped with multiple phosphors and a 365 nm UV-LED, have achieved the best white light quality reported to date in the literature. These devices also show great thermal and power spectral stability as well as excellent CCT tunability from warm white (3000 K) to cold white (6000 K), while maintaining both high CRI (R_a) and R9 values. Our work opens up a new route toward next-generation solid-state lighting devices with superior color quality.

■ ASSOCIATED CONTENT

Supporting Information

The Supporting Information is available free of charge on the ACS Publications website at DOI: 10.1021/acsami.8b12474.

Experimental methods, UV–vis absorption spectra, photophysical properties of phosphors, PLQE comparison of ball-milled powders and single crystals, table of white light simulation results, temperature-dependent photo luminescence, CIE 1931 diagram showing chromaticity points under forward bias current variation and high-temperature aging, current efficiency and EQE of prototype WLED (PDF)

■ AUTHOR INFORMATION

Corresponding Author

*E-mail: bma@fsu.edu (B.M.).

ORCID

Yan Zhou: 0000-0002-7290-1401

Biwu Ma: 0000-0003-1573-8019

Funding

National Science Foundation (NSF) (DMR-1709116) and the Air Force Office of Scientific Research (AFOSR) (17RT0906)

DOI: 10.1021/acsami.8b12474
ACS Appl. Mater. Interfaces 2018, 10, 30051–30057

Notes

The authors declare no competing financial interest.

■ ACKNOWLEDGMENTS

The authors acknowledge the funding support from the National Science Foundation (NSF) (DMR-1709116) and the Air Force Office of Scientific Research (AFOSR) (17RT0906).

■ REFERENCES

(1) George, N. C.; Denault, K. A.; Seshadri, R. Phosphors for Solid-State White Lighting. *Annu. Rev. Mater. Res.* **2013**, *43*, 481−501.
(2) Cho, J.; Park, J. H.; Kim, J. K.; Schubert, E. F. White Light-Emitting Diodes: History, Progress, and Future. *Laser Photonics Rev.* **2017**, *11*, 1600147.
(3) Tosini, G.; Ferguson, I.; Tsubota, K. Effects of Blue Light on the Circadian System and Eye Physiology. *Mol. Vis.* **2016**, *22*, 61−72.
(4) Kimura, N.; Sakuma, K.; Hirafune, S.; Asano, K.; Hirosaki, N.; Xie, R. J. Extrahigh Color Rendering White Light-Emitting Diode Lamps Using Oxynitride and Nitride Phosphors Excited by Blue Light-Emitting Diode. *Appl. Phys. Lett.* **2007**, *90*, 051109.
(5) Fukui, T.; Kamon, K.; Takeshita, J.; Hayashi, H.; Miyachi, T.; Uchida, Y.; Kurai, S.; Taguchi, T. Superior Illuminant Characteristics of Color Rendering and Luminous Efficacy in Multilayered Phosphor Conversion White Light Sources Excited by Near-Ultraviolet Light-Emitting Diodes. *Jpn. J. Appl. Phys.* **2009**, *48*, 112101.
(6) Kwon, K. H.; Im, W. B.; Jang, H. S.; Yoo, H. S.; Jeon, D. Y. Luminescence Properties and Energy Transfer of Site-Sensitive $Ca_{6-x-y}Mg_{x-z}(PO_4)_4:Eu_y^{2+},Mn_z^{2+}$ Phosphors and Their Application to Near-UV LED-Based White LEDs. *Inorg. Chem.* **2009**, *48*, 11525−11532.
(7) Ruan, C.; Bai, X.; Sun, C.; Chen, H. B.; Wu, C. F.; Chen, X. B.; Chen, H. D.; Colvin, V. L.; Yu, W. W. White Light-Emitting Diodes of High Color Rendering Index With Polymer Dot Phosphors. *RSC Adv.* **2016**, *6*, 106225−106229.
(8) Wang, Z.; Yuan, F.; Li, X.; Li, Y.; Zhong, H.; Fan, L.; Yang, S. 53% Efficient Red Emissive Carbon Quantum Dots for High Color Rendering and Stable Warm White-Light-Emitting Diodes. *Adv. Mater.* **2017**, *29*, 1702910.
(9) Smet, P. F.; Parmentier, A. B.; Poelman, D. Selecting Conversion Phosphors for White Light-Emitting Diodes. *J. Electrochem. Soc.* **2011**, *158*, R37−R54.
(10) Ye, S.; Xiao, F.; Pan, Y. X.; Ma, Y. Y.; Zhang, Q. Y. Phosphors in Phosphor-Converted White Light-Emitting Diodes: Recent Advances in Materials, Techniques and Properties. *Mater. Sci. Eng., R* **2010**, *71*, 1−34.
(11) Narukawa, Y.; Niki, I.; Izuno, K.; Yamada, M.; Murazaki, Y.; Mukai, T. Phosphor-Conversion White Light Emitting Diode Using InGaN Near-Ultraviolet Chip. *Jpn. J. Appl. Phys., Part 2* **2002**, *41*, L371−L373.
(12) Sivakumar, V.; Varadaraju, U. V. Synthesis, Phase Transition and Photoluminescence Studies on Eu^{3+}-Substituted Double Perovskites—A Novel Orange-Red Phosphor for Solid-State Lighting. *J. Solid State Chem.* **2008**, *181*, 3344−3351.
(13) Xie, R. J.; Hirosaki, N.; Mitomo, M. Oxynitride/Nitride Phosphors for White Light-Emitting Diodes (LEDs). *J. Electroceram.* **2008**, *21*, 370−373.
(14) He, X. H.; Lian, N.; Sun, J. H.; Guan, M. Y. Dependence of Luminescence Properties on Composition of Rare-Earth Activated (Oxy)Nitrides Phosphors for White-LEDs Applications. *J. Mater. Sci.* **2009**, *44*, 4763−4775.
(15) Dai, Q.; Foley, M. E.; Breshike, C. J.; Lita, A.; Strouse, G. F. Ligand-Passivated $Eu:Y_2O_3$ Nanocrystals as a Phosphor for White Light Emitting Diodes. *J. Am. Chem. Soc.* **2011**, *133*, 15475−15486.
(16) Kaczmarek, A. M.; Van Deun, R. Rare Earth Tungstate and Molybdate Compounds - From 0D to 3D Architectures. *Chem. Soc. Rev.* **2013**, *42*, 8835−8848.
(17) Li, F.; Nie, C.; You, L.; Jin, X.; Zhang, Q.; Qin, Y.; Zhao, F.; Song, Y.; Chen, Z.; Li, Q. White Light Emitting Device Based on Single-Phase CdS Quantum Dots. *Nanotechnology* **2018**, *29*, 205701.
(18) Sun, Y. P.; Zhou, B.; Lin, Y.; Wang, W.; Fernando, K. A.; Pathak, P.; Meziani, M. J.; Harruff, B. A.; Wang, X.; Wang, H.; Luo, P. G.; Yang, H.; Kose, M. E.; Chen, B.; Veca, L. M.; Xie, S. Y. Quantum-Sized Carbon Dots for Bright and Colorful Photoluminescence. *J. Am. Chem. Soc.* **2006**, *128*, 7756−7757.
(19) Lim, J.; Jun, S.; Jang, E.; Baik, H.; Kim, H.; Cho, J. Preparation of Highly Luminescent Nanocrystals and Their Application to Light-Emitting Diodes. *Adv. Mater.* **2007**, *19*, 1927−1932.
(20) Ziegler, J.; Xu, S.; Kucur, E.; Meister, F.; Batentschuk, M.; Gindele, F.; Nann, T. Silica-Coated InP/ZnS Nanocrystals as Converter Material in White LEDs. *Adv. Mater.* **2008**, *20*, 4068−4073.
(21) Lita, A.; Washington, A. L.; van de Burgt, L.; Strouse, G. F.; Stiegman, A. E. Stable Efficient Solid-State White-Light-Emitting Phosphor With a High Scotopic/Photopic Ratio Fabricated from Fused CdSe-Silica Nanocomposites. *Adv. Mater.* **2010**, *22*, 3987−3991.
(22) Jo, D. Y.; Yang, H. Synthesis of Highly White-Fluorescent Cu-Ga-S Quantum Dots for Solid-State Lighting Devices. *Chem. Commun. (Cambridge, U. K.)* **2016**, *52*, 709−712.
(23) Findlay, N. J.; Bruckbauer, J.; Inigo, A. R.; Breig, B.; Arumugam, S.; Wallis, D. J.; Martin, R. W.; Skabara, P. J. An Organic Down-Converting Material for White-Light Emission from Hybrid LEDs. *Adv. Mater.* **2014**, *26*, 7290−7294.
(24) Di Martino, D.; Beverina, L.; Sassi, M.; Brovelli, S.; Tubino, R.; Meinardi, F. Straightforward Fabrication of Stable White LEDs by Embedding of Inorganic UV-LEDs into Bulk Polymerized Polymethyl-methacrylate Doped With Organic Dyes. *Sci. Rep.* **2015**, *4*, 4400.
(25) Huang, H.; Chen, B. K.; Wang, Z. G.; Hung, T. F.; Susha, A. S.; Zhong, H. Z.; Rogach, A. L. Water Resistant $CsPbX_3$ Nanocrystals Coated With Polyhedral Oligomeric Silsesquioxane and Their Use as Solid State Luminophores in All-Perovskite White Light-Emitting Devices. *Chem. Sci.* **2016**, *7*, 5699−5703.
(26) Palazon, F.; Di Stasio, F.; Akkerman, Q. A.; Krahne, R.; Prato, M.; Manna, L. Polymer-Free Films of Inorganic Halide Perovskite Nanocrystals as UV-to-White Color-Conversion Layers in LEDs. *Chem. Mater.* **2016**, *28*, 2902−2906.
(27) Sun, C.; Zhang, Y.; Ruan, C.; Yin, C.; Wang, X.; Wang, Y.; Yu, W. W. Efficient and Stable White LEDs With Silica-Coated Inorganic Perovskite Quantum Dots. *Adv. Mater.* **2016**, *28*, 10088−10094.
(28) Wang, P.; Bai, X.; Sun, C.; Zhang, X. Y.; Zhang, T. Q.; Zhang, Y. Multicolor Fluorescent Light-Emitting Diodes Based on Cesium Lead Halide Perovskite Quantum Dots. *Appl. Phys. Lett.* **2016**, *109*, 063106.
(29) Zhang, M.; Wang, M. Q.; Yang, Z.; Li, J. J.; Qiu, H. W. Preparation of All-Inorganic Perovskite Quantum Dots-Polymer Composite for White LEDs Application. *J. Alloys Compd.* **2018**, *748*, 537−545.
(30) Lorbeer, C.; Mudring, A. V. White-Light-Emitting Single Phosphors via Triply Doped LaF_3 Nanoparticles. *J. Phys. Chem. C* **2013**, *117*, 12229−12238.
(31) Kundu, J.; Ghosh, Y.; Dennis, A. M.; Htoon, H.; Hollingsworth, J. A. Giant Nanocrystal Quantum Dots: Stable Down-Conversion Phosphors that Exploit a Large Stokes Shift and Efficient Shell-to-Core Energy Relaxation. *Nano Lett.* **2012**, *12*, 3031−3037.
(32) Jang, E.; Jun, S.; Jang, H.; Lim, J.; Kim, B.; Kim, Y. White-Light-Emitting Diodes With Quantum Dot Color Converters for Display Backlights. *Adv. Mater.* **2010**, *22*, 3076−3080.
(33) Zhao, B. X.; Zhang, D. L.; Sun, K.; Wang, X. B.; Mao, R. H.; Li, W. W. Intrinsic Quantum Dot Based White-Light-Emitting Diodes With a Layered Coating Structure for Reduced Reabsorption of Multiphase Phosphors. *RSC Adv.* **2014**, *4*, 45155−45158.
(34) Wang, X.; Yan, X.; Li, W.; Sun, K. Doped Quantum Dots for White-Light-Emitting Diodes Without Reabsorption of Multiphase Phosphors. *Adv. Mater.* **2012**, *24*, 2742−2747.

DOI: 10.1021/acsami.8b12474
ACS Appl. Mater. Interfaces 2018, 10, 30051−30057

(35) Zhou, C. K.; Lin, H. R.; Tian, Y.; Yuan, Z.; Clark, R.; Chen, B. H.; van de Burgt, L. J.; Wang, J. C.; Zhou, Y.; Hanson, K.; Meisner, Q. J.; Neu, J.; Besara, T.; Siegrist, T.; Lambers, E.; Djurovich, P.; Ma, B. W. Luminescent Zero-Dimensional Organic Metal Halide Hybrids With Near-Unity Quantum Efficiency. *Chem. Sci.* **2018**, *9*, 586−593.
(36) Zhou, C. K.; Tian, Y.; Yuan, Z.; Lin, H. R.; Chen, B. H.; Clark, R.; Dilbeck, T.; Zhou, Y.; Hurley, J.; Neu, J.; Besara, T.; Siegrist, T.; Djurovich, P.; Ma, B. W. Highly Efficient Broadband Yellow Phosphor Based on Zero-Dimensional Tin Mixed-Halide Perovskite. *ACS Appl. Mater. Interfaces* **2017**, *9*, 44579−44583.
(37) Zhou, C. K.; Worku, M.; Neu, J.; Lin, H. R.; Tian, Y.; Lee, S. J.; Zhou, Y.; Han, D.; Chen, S. Y.; Hao, A.; Djurovich, P. I.; Siegrist, T.; Du, M. H.; Ma, B. W. Facile Preparation of Light Emitting Organic Metal Halide Crystals with Near-Unity Quantum Efficiency. *Chem. Mater.* **2018**, *30*, 2374−2378.
(38) Xu, L. J.; Sun, C. Z.; Xiao, H.; Wu, Y.; Chen, Z. N. Green-Light-Emitting Diodes based on Tetrabromide Manganese(II) Complex Through Solution Process. *Adv. Mater.* **2017**, *29*, 1605739.
(39) Kim, K. B.; Kim, Y. I.; Chun, H. G.; Cho, T. Y.; Jung, J. S.; Kang, J. G. Structural and Optical Properties of $BaMgAl_{10}O_{17}$: Eu^{2+} Phosphor. *Chem. Mater.* **2002**, *14*, 5045−5052.
(40) Davis, W.; Ohno, Y.Toward an Improved Color Rendering Metric. In *SPIE International Conference on Solid State Lighting*; SPIE: Bellingham, WA, 2005; Vol. *5941*.
(41) McKittrick, J.; Shea-Rohwer, L. E. Review: Down Conversion Materials for Solid-State Lighting. *J. Am. Ceram. Soc.* **2014**, *97*, 1327−1352.
(42) Ohno, Y. Spectral design considerations for white LED color rendering. *Opt. Eng.* **2005**, *44*, 111302.
(43) Bizarri, G.; Moine, B. On $BaMgAl_{10}O_{17}$: Eu^{2+} Phosphor Degradation Mechanism: Thermal Treatment Effects. *J. Lumin.* **2005**, *113*, 199−213.
(44) Schubert, E. F.; Kim, J. K. Solid-State Light Sources Getting Smart. *Science* **2005**, *308*, 1274−1278.
(45) Forrest, S. R.; Bradley, D. D. C.; Thompson, M. E. Measuring the Efficiency of Organic Light-Emitting Devices. *Adv. Mater.* **2003**, *15*, 1043−1048.

DOI: 10.1021/acsami.8b12474
ACS Appl. Mater. Interfaces 2018, 10, 30051−30057